Chapter 3

Giant Magnetoresistance and $I-V$ Asymmetries in Nickel Magnetic Point Contacts

3.1 Introduction

The use of the GMR effect in industrial applications has already led to the construction of the present generation of magnetic data storage devices. However, in order to reach storage densities of the order of Terabit/in^2 a substantial down-scaling of the read/write devices is needed. One possible avenue to this target is given by magnetic point contacts (MPC's), where the lateral size of the typical contacts approaches the atomic scale.

Recent experiments have shown that nanoscaled magnetic point contacts may present huge magnetoresistance (HGMR) [11, 12, 162, 168, 184, 169] reaching up to a few hundred thousand percent (using the optimistic definition of MR). This result alone can be seen as a major leap toward nanoscopic magnetic memory read/write devices. In addition, it is important to report that electro-deposited nickel point contacts present highly asymmetric I-V characteristics typical of a diode-like behaviour [184, 169]. A complete explanation of both these effects is still lacking.

To date there is a large debate around the origin of the large magnetoresistance effects in MPC's. On the one hand, it has been argued that magnetic field-induced mechanical effects can produce a large GMR (LGMR) - $\sim$ 100 - 500 %. In fact, either magnetostriction, dipole-dipole interactions between the apexes [185] and magnetically induced stress relief [186] may have the effect of compressing the nanocontact once a magnetic field is applied. This enlarges the cross section of the MPC and consequently the resistance of the junction decreases. On the other hand, there are also strong indications that mechanical effects alone are not able to account for whole

magnetoresistance. Specifically García *et. al.* have shown that the behaviour of MPC's does not comply with mechanical changes, in particular with magnetostriction effects [11, 162].

In our opinion, three important works demonstrated that LGMR in magnetic point contacts can be attributed to an electronic origin. First van Hoof *et. al.* [187] showed that the resistance of an abrupt domain wall (DW) can be rather large, giving rise to a GMR of the order of 60%. The calculations were performed using realistic band-structure for Stoner ferromagnets (Fe, Ni and Co) and the current was calculated in linear response limit. Along the same lines Tatara *et. al.* [188] demonstrated that later confinement can enhance the GMR. In this work values of the order of 300% were obtained in ultra-small point contacts, in good agreement with experiments. Finally, Bruno [167] demonstrated that if the magnetic moments on the apexes of a magnetic constriction are not aligned parallel to each then a DW will be formed inside the constricted region. The main features of this DW are quite different from those of the well know Bloch [103, 189] and Néel [104] walls. In particular, the crucial point is that the length of the DW is predicted to be as long as the diameter of the constriction. This result suggests that the DW trapped in an atomic scale MPC may be very sharp, only a few atomic planes long. At this length scales a DW produces a rather strong spin-dependent scattering potential and large magneto-induced effects are somehow expected. In this context it is important to report that such an extreme confinement has been already achieved by contacting two magnetic grains with different orientation [168]. Unfortunately, these theoretical predictions are unable to account for HGMR. The MR values are usually two or three orders of magnitude lower even in the best case scenario (largest scattering).

Since these seminal works, a number of theoretical works on transport through magnetic domain walls have been presented [190, 191, 192]. These, as well as the two previously mentioned, consider equilibrium transport in the spirit of the Landauer-Büttiker formalism [84]; current induced effects such as charging of the point contact and, quite possibly, movement of the domain wall have not been taken into consideration. However, in low dimensional systems such as MPCs the introduction of small biases might cause charge accumulation inside the MPC, changing its transport properties [193].

The aim of this chapter is to provide a fully quantitative description of the origins of the reported LGMR and HGMR values and to understand whether they arise solely from electronic mechanisms. In order to do so one must consider an accurate description of the electronic structure of these MPCs which lead us into DFT-based

Hamiltonians and ultimately to *Smeagol*. *Smeagol* was used to calculate the zero bias transmission probabilities of different atomic and magnetic configurations of our system.

Recently it has been suggested that the presence of oxygen in Ni MPCs could lead to HGMR [163]. This suggestion follows from the insulating ground state of bulk NiO. Therefore it is also interesting to address the issue of impurities in the MPCs and their effects on the transport properties.

In all cases we model the magnetoresistance in MPC using the typical spin-valve scheme: we assume that in the absence of a magnetic field, the magnetisation vectors of the two leads are aligned opposite to each other - antiparallel alignment (AA). Therefore in the zero field situation a sharp DW is formed inside the MPC. Then, when a magnetic field is applied, the magnetic moments of the leads align parallel to each other and the wall is eliminated - parallel alignment (PA).

Furthermore we only consider collinear spins. This is justified by a recent calculation from Imamura *et. al.* [190] who have used a Heisenberg model in a mean field approximation to show that, in the case of a domain wall pinned in a constriction, there is no spin precession and minority and majority bands can be treated separately.

3.2 Magnetoresistance in Nickel point contacts: an *ab initio* study

Hence the question raised in section (3.1) of this chapter still remains: is it possible to obtain huge giant-magnetoresistance (in excess of 100,000 %) solely from electronic effects [11, 162, 168, 184] ?

In order to address this raised in section (3.1), we need to model our point contact using a realistic description of the electronic structure while choosing an atomic arrangement that best describes the experimental conditions. *Smeagol* is the ideal tool for this task.

In the case of atomically thin Ni MPCs, Viret *et al.* have shown by molecular dynamics simulations that the last step in the stretching of a Ni break junction experiment forms two Ni pyramids joined at the neck by two atoms, without forming a single atom chain [164]. This particular configuration is shown in Fig. (3.1). Transmission electron microscopy experiments have confirmed that metallic quantum point contacts retain their crystallographic arrangement even at the limit of atomically thin junctions for a range of different metals [151, 154, 92, 157, 173]. Hence,

the two pyramids maintain the bulk lattice structure.

3.2.1 Impurity-free MPCs: relaxation and transport I

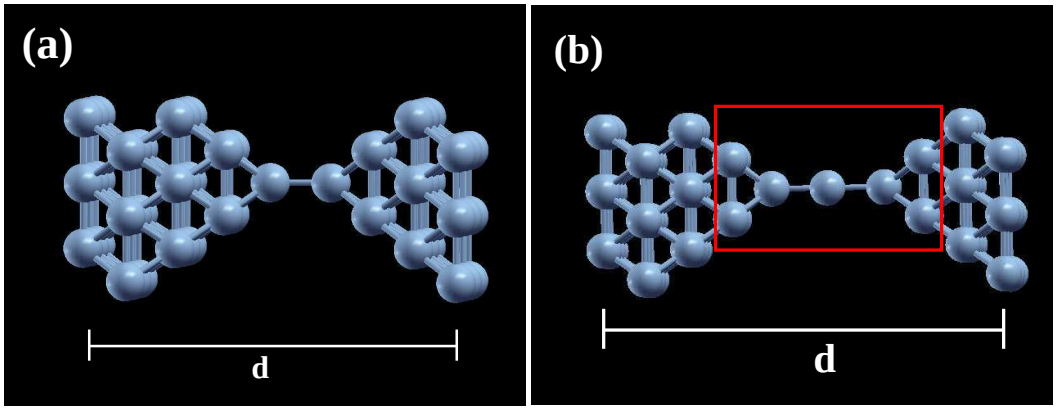

Figure 3.1: Ball-and-stick representation of a nickel point contact formed by two pyramidal tips joined together. a) The pyramid are directly connected at the end points (MPC-2), b) the tips are bridged together by a single atom (MPC-3). The eleven atoms enclosed in the red rectangle correspond to the tip atoms (three atoms forming the atomic chain and four atoms on either side forming the apexes.

Our simulations are performed on atomic size point contacts with an arrangement similar to those proposed by Viret *et al.* [164]. The structure of a Ni break junction close to the rupture point is modelled as two Ni pyramids oriented along the [001] direction. At first, the geometry of the two tips follows the crystallographic structure of fcc bulk Ni as obtained by DFT.[1] We considered two possible cases: 1) the tips are directly bridged together (MPC-2 geometry) or 2) one nickel atom is place between the two pyramids to form a single-atom chain (MPC-3). These two arrangements are shown in figure (3.1). The structures consist of 55 and 56 nickel atoms respectively.

The equilibrium position of the Ni atoms are expected to change due to relaxations (specially for the atoms closest to and at the tip). Hence we performed structure relaxations of the MPCs using SIESTA to obtain the lowest energy arrangement for both configurations. The atoms are allowed to relax following standard conjugate gradient (CG) methods [40]. Two of the left-most and two of of the right-most planes were kept fixed at the Ni fcc bulk positions, while the middle atoms are free to move. Once convergence for a particular arrangement is obtained we then increase the size

[1] Lattice constant a $\sim$ 3.46 Å.

of the cell, d (the distance between the pyramids along the z direction) by slightly separating the planes. Then another relaxation if performed.

The basis set is chosen as a double-ζ (DZ) s with polarised orbitals and a double-ζ p and d.[2] The resulting total energy curve as a function of the cell size is presented in figure (3.2).[3] In both cases there we can see a clear energy minimum. Hereafter, all the calculations shown were performed using the relaxed coordinates at this energy minimum.

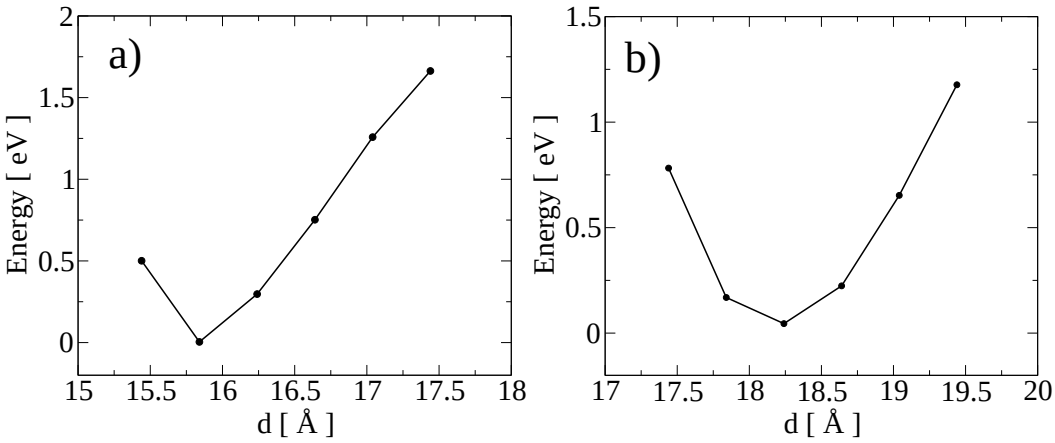

Figure 3.2: Total energy curves for different tip separations in the a) MPC-2 and b) MPC-3 structures shown in Fig. (3.1)). The atoms in the central region are allowed to relax while the last two slices to the left and to the right are kept at fixed coordinates. The positions of the atoms at the apexes are kept at their respective bulk fcc arrangement. The tips are oriented along the [001] direction.

The projected density of states (PDOS) can provide some insight into the character the states lying close to the Fermi level. In figure (3.3) we present the density of states projected onto the s and d orbitals of the entire MPC and the PDOS of the tip atoms. We can see that the density of states for the entire MPC is similar to the one of the apexes (four atoms to the left and to the right of the three-atom chain), but for a scaling factor (which account for the number of atoms in the relative region). It clearly resembles the density of states of bulk nickel. On the other hand, the PDOS for the three-atom chain (Fig. (3.3d)) clearly shows the effects of low-coordination, the density of states is much sharper than in the rest of the MPC (and in that of bulk). This in turn will result in some sharp features in the transmission probabilities of the point contact, specially for minority spins.

[2]Note that the p orbitals used here are not semi-core states, but the $4p$ orbital of Ni (empty valence orbitals).

[3]Our relaxations are performed in a collinear ferromagnetic alignment. We have assumed that

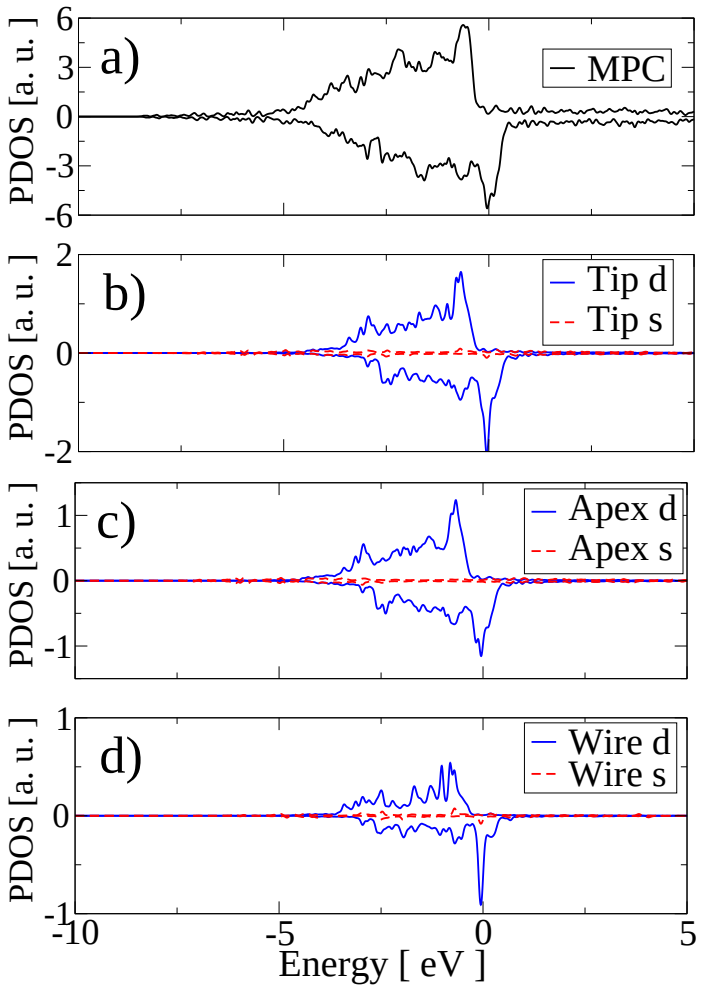

Figure 3.3: Projected density of states for the MPC-3 structure in figure (3.1b). a) Whole MPC, b) 11 atoms in the central region, three atoms forming the wire and four apex atoms on either side (shown inside the red box in Fig. (3.1b). c) Apex atoms on the left and on the right. d) The 3 Ni atoms in the monoatomic chain.

The low bias magnetoresistance values for these MPCs can be obtained by calculating the zero-bias transmission coefficients. Figure (3.4) shows the energy-dependent transmission coefficients for the parallel (a) and anti-parallel (b) spin configurations of the MPC-2 arrangement.

We can clearly see that in the parallel configuration the conductance at the Fermi level is dominated by the minority spins (G $\sim$ 2.5 G_0) whereas the conductance for the majority lies close to 1 G_0. This behaviour can be explained by the presence

magnetic contributions to the forces will not significantly influence the final structure.

of partially empty d states at the Fermi level for the minority spins and completely filled states below the Fermi energy for the majority. At energies $(E - E_F) > 0$, the conductance is governed by the unpolarised s orbitals and it is quite similar for both up and down spins. For s orbitals one would expect a single channel for each spin component, but given the small distance between the pyramids we also observe direct transmission across the apexes of the pyramids, hence a larger conductance. In the anti-parallel case the system the DW is positioned between the two tips, so we see a mirror symmetric system and the transmission coefficients for majority and minority spins are identical. The GMR ratio for the MCP-2 was calculated to be approximately -5 % . Note that the GMR is not only very small, but also negative. This means that the conductance in the anti-parallel case is higher than that in the parallel one.

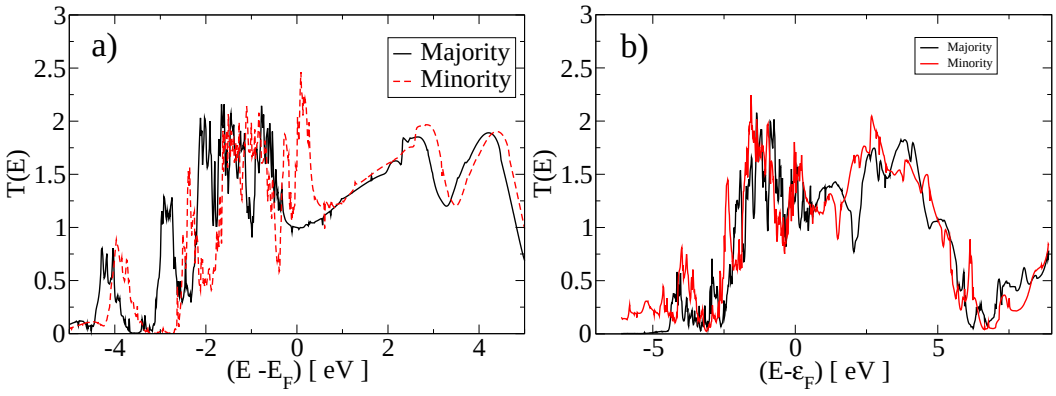

Figure 3.4: Transmission coefficients as a function of energy for Ni point contacts for the MPC-2 structure in the (a) parallel and (b) anti-parallel configuration. The majority (minority) spins are represented by solid (dashed) lines.

For the single-atom chain the picture changes slightly. Figure (3.5) shows the transmission coefficients for the MPC-3 as a function of energy. In the PA configuration we still see minority-dominated transmission, but with a slightly higher conductance. Most importantly, the introduction of an extra atom drastically reduces the conductance above the Fermi level corroborating our interpretation of direct transmission across the pyramids. In fact, we see a reasonably flat plateau around 1 G_0 for $\epsilon > E_F$, a contribution from the unpolarised s electrons. In the AA configuration we placed the DW between he first and the second atom of the chain, hence the symmetry is broken. The GMR for this case is slightly higher (~ 20 %).

Unfortunately, in both cases presented here s electrons strongly contribute to the transmission coefficients for both majority and minority spins. The presence of nearly

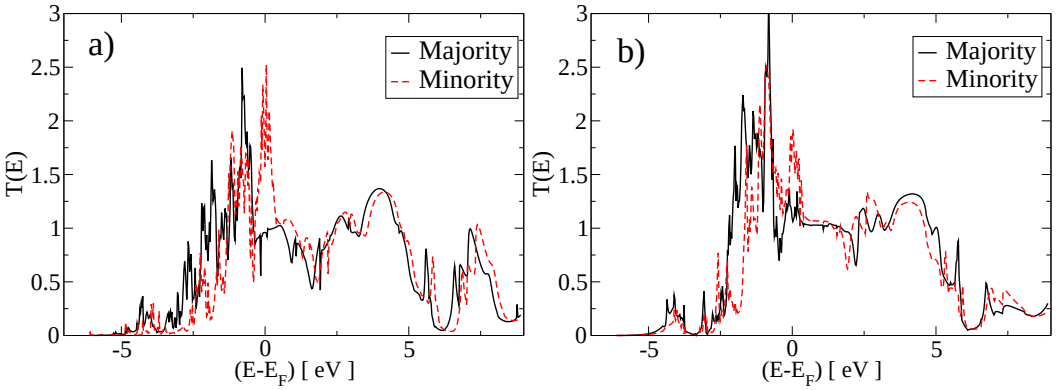

Figure 3.5: Transmission coefficients as a function of energy for Ni point contacts for a single atom chain in the (a) parallel and (b) anti-parallel configuration. The majority (minority) spins are represented by solid black (dashed red) lines.

unpolarised s orbitals set an inherent limit to the GMR in magnetic multilayers too. Therefore, so far, our results seem to indicate that huge magnetoresistance (or even just LGMR) effects are not possible in these systems.

3.2.2 Effects of different exchange-correlation potentials (V_{XC}) in impurity-free Ni point contacts

Although extremely useful in many cases, the LDA (and GGA) gives poor results for a variety of systems, specially those where strong correlation effects are important. Albeit bulk Ni does not figure in this class of problems (in fact, properties such as the magnetic moment are extremely well described by LDA), the same cannot be said about low-coordinated systems such as atomic-size chains.

In transition metals the d orbitals figure close to or at the Fermi level. The bands formed by these atoms are highly directional and in an one-dimensional system, one would expect a lift of the degeneracy. Let's take an infinite Ni chain for example. In figure (3.6) we present a schematic representation of the d orbitals in an mono-atomic wire. While orbitals d_{z^2}, d_{yz} and d_{xz} are oriented along the chain, orbitals d_{xy} and $d_{x^2-y^2}$ are perpendicular to it axis. Because d orbitals are quite short the coupling between adjacent orbitals, in the case of d_{xy} and $d_{x^2-y^2}$, is rather small which in turn will lead to localisation and strong $e-e$ interaction.[4]

Hence, in order to describe the electronic structure it is necessary to use exchange and correlation functionals which account for strong correlation. Unfortunately, most

[4]Note that in noble metals such as gold and silver the valence orbitals have s character which do not have any angular dependence. One would expect in this case LDA to yield a good description of the atomic chains (see section (2.5.2)).

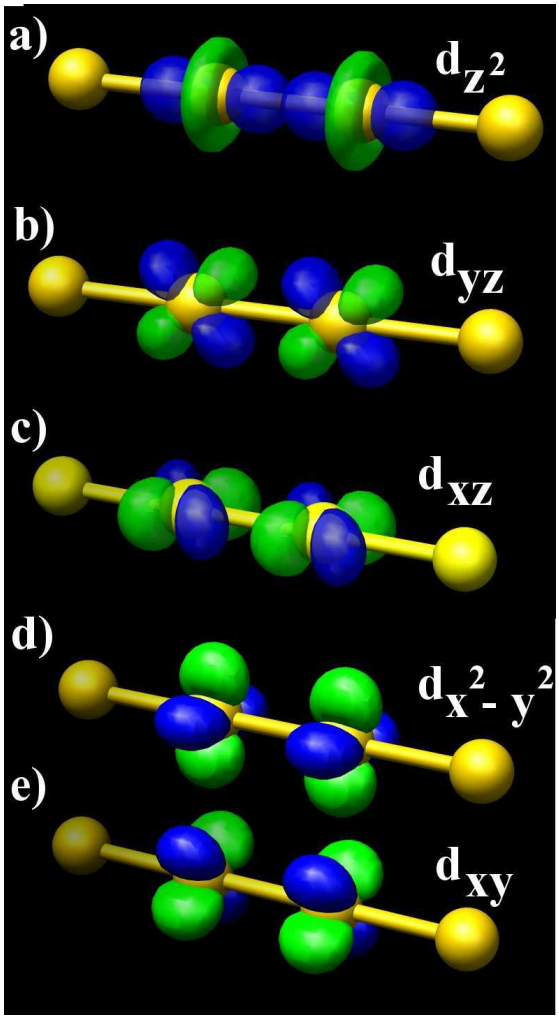

Figure 3.6: Schematic representation of the atomic orbitals in an infinite Ni mono-atomic wire oriented along z. a) d_{z^2}, b) d_{yz}, c) d_{xz}, d) $d_{x^2-y^2}$ and e) d_{xy}. The $d_{x^2-y^2}$ and d_{xy} are perpendicular to the axis of the wire and therefore weakly coupled.

functionals that correct over LDA tend to over-correct metallic systems, where usually LDA gives good results. The problem then becomes that of finding a good functional for the low connectivity apex region which does not alter the electronic structure of the planes at the edges of the cell which resemble bulk Ni.

The LDA+U is particularly suited for this purpose. Albeit based on empirical parameters one can choose to correct a set of d orbitals on a particular group of atoms preserving the LDA description for the rest of the system. The LDA+U functional was implemented in SIESTA [132] and Smeagol [85].

In order to gauge the effect of the LDA+U approximation on the transport prop-

erties we first performed calculations on an infinite one-dimensional nickel chain. This way we find the values of U and J for which the band structure of our chain is correctly described. We consider a linear chain of Nickel atoms $\sim$ 2.24 Å apart oriented along the z direction and in the ferromagnetic alignment. This lattice spacing corresponds to the approximate interatomic distance between atoms in the three atom chain of the MPC. We then performed calculations using different types of exchange-correlation potentials namely: standard LSDA, LDA+U [132] and ASIC. The latter was implemented in SIESTA by Pemmaraju *et al.* [86].

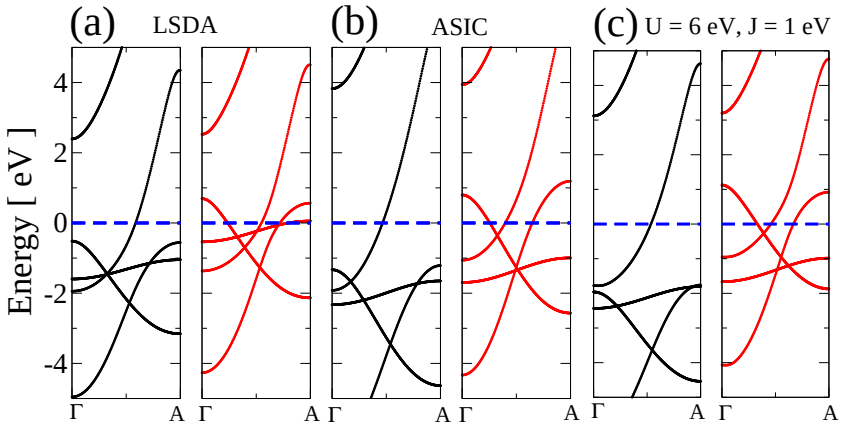

Figure 3.7: Band structures around the Fermi level for a one-dimensional infinite nickel chain. a) LSDA, c) atomic self-interaction correction and c) LDA+U with U=6 eV and J=1 eV. The black (red) curves correspond to majority (minority) spin bands.

Atomic SIC, which is fully *ab initio* (it does not require empirical parameters) was taken as our benchmark for LDA+U. In figure (3.7) we present the band structure along the chain axis and demonstrate the effects of low dimensionality on Nickel. When compared to standard LSDA, we can clearly see that the more localised filled d bands are shifted down in energy, away from the Fermi level; more prominently the minority d_{xy} and $d_{x^2-y^2}$ states which are perpendicular to chain axis and present a very loose interatomic coupling lie close to the Fermi level for LSDA and are shifted downwards in ASIC and LDA+U.

Comparing our calculations for LDA+U and ASIC we can settle on a set of values for U and J which correctly describe the band structure of the infinite chain including corrections for the occupied orbitals,

$$U = 6 \text{ eV} \quad , \quad J = 1 \text{ eV}. \tag{3.1}$$

These values were used for all our calculations.

We assume that the atomic arrangement is not significantly affected by the Hubbard-U correction over LDA, hence we have kept the same arrangement from the previous section (Fig. (3.1)). The transmission coefficients as a function of energy for the MPC-3 are shown in figure (3.8). From the figure we can we see that the total transmission in the PA close to the Fermi level is enhanced (particularly for minority spins) compared to the LSDA calculation presented in the previous section. We can also see that the transmission for the majority spins is close to unity for a wide range of energies indicating less hybridisation between s and d states. This is also clear when see that the conductance due to d orbitals starts to play a role at lower energies when compared to our LSDA calculations.

The results for the parallel case can be directly correlated to the band structures of figure (3.7). The majority spins present a single broad s band (the first d band is approximately 3 eV below). For the minority spins there is a doubly degenerate d state (d_{yz} and d_{xz}) and one hybridised $s - d_{z^2}$ state (note the anti-crossing at the Fermi level) which in turn results in a conductance of about 2.5 G_0.

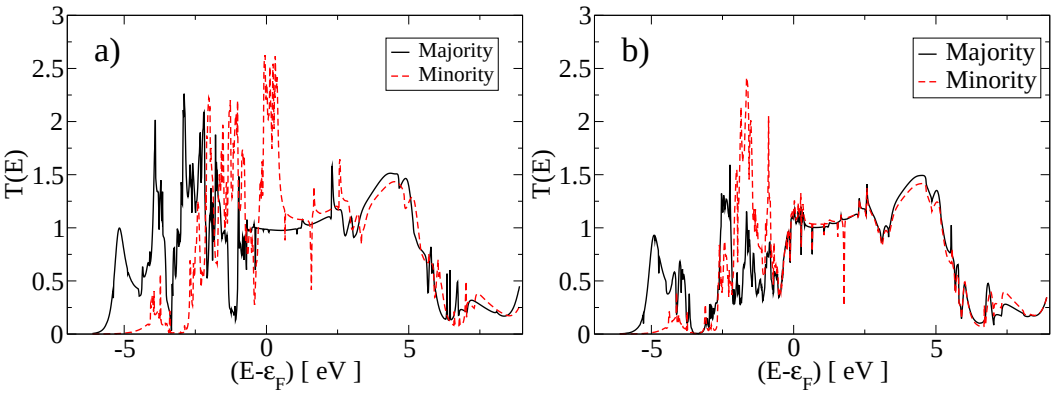

Figure 3.8: Transmission coefficients as a function of energy using LDA+U for Ni point contacts with using LDA+U. (a) Parallel and (b) anti-parallel cases for the single-long chain. The values of U and J were set to 6 eV and 1 eV respectively.

We can also use Fig. (3.7) to understand the AA. Let us assume that the three atom chain can be considered as two semi-infinite Ni wires separated by a DW. In that case the band structure on the right-hand-side is swapped (up spins $\rightleftharpoons$ down spins) compared to the left-hand-side one. For Minority spins coming from the left have three open channels: one hybridised $s-d_{z^2}$ band and the degenerate d_{yz} and d_{xz} orbitals. When they flow across the domain wall they must propagate as majority states. For majority spins there is only a single sd_{z^2} band. Hence the other two states Bloch states are completely backscattered and the transmission is approximately 1

G_0. Moreover, if electrons are coming from the left on the majority spin channel there is only one accessible band at the Fermi level which is also available for minority spins once the electrons flow across the DW. Hence, for both up and down spins this simple picture gives a conductance of 1 G_0.

The total GMR in this case goes up considerably to approximately 60 %, in agreement with similar calculations using performed with alternative *ab initio* methods [194, 195]. However, this value is at least two orders of magnitude smaller than the ones observed in some of the experiments where HGMR was measured [11, 162, 168].

Although LDA+U significantly changes the electronic structure of the wire close to the Fermi level, the overall effect on the transmission coefficients is not enough to give rise to HGMR. This is mostly because the d_{xy} and $d_{x^2-y^2}$ bands which are removed from the Fermi level when we use LDA+U have little of no influence on the transport properties of the MPC.

On one hand, the GMR values obtained above show that it is possible to have useful nanoscale spintronics devices. We have observed that it is possible to obtain GMR in atomic point contacts with a magnetoresistance ratio at least similar to that of multilayer materials. This can lead to smaller technology preserving the same sensitivity of standard read/write heads in computer hard drives. On the other hand, despite larger GMR ratios, the introduction of the LDA+U exchange-correlation functional to correct for localisation does not qualitatively change the picture. Most notably, we have been unable to account for HGMR from solely electronic arguments. This is mostly because the d_{xy} and $d_{x^2-y^2}$ bands which are removed from the Fermi level when we use LDA+U have little of no influence on the transport properties of the MPC.

Hence, one must conclude that impurity free MPCs do not present HGMR for the arrangements we have studied. Other mechanisms might be playing a role. One possibility is that impurities are present in the MPC.

3.2.3 Oxygen-rich MPCs: relaxation and transport II

Recently García *et al.* [163] have proposed that the presence of impurities, in particular oxygen might be related to HGMR (values exceeding 1,000 %). These experiments are performed in air, but it is observed that even experiments in ultra high vacuum conditions can become contaminated after a couple of hours [92]. Therefore, it is reasonable to speculate that impurity atoms may be lying close to the constricted region in MPCs. It is also very likely that at the atomic scale even a single impurity may have a large effect on the current flowing through the device.

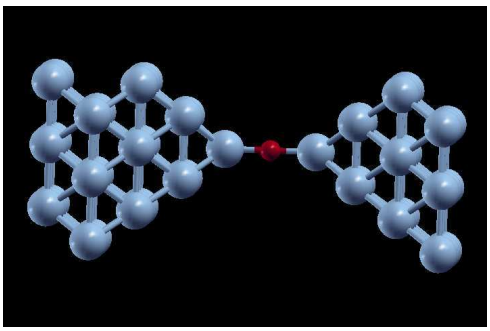

Figure 3.9: Ball-and-stick representation of the converged atomic arrangement of a nickel point contact with one oxygen atom bridging the gap between the two tips. Colour code: blue - Ni; red - O.

It is also well know that Ni is extremely reactive to oxygen and that bulk NiO is an insulator. If we position a single oxygen impurity bridging the two Ni [001] pyramids, the central region will resemble a one-dimensional NiO nanowire. If this system is insulating as its bulk counterpart it is possible that the contribution coming from the non-spin-polarised s bands will be removed from the Fermi level. In turn, this could lead larger MR ratios. In many aspects this 1D systems is the smallest conceivable tunnelling junction.

Tunnelling junctions are made of two magnetic layers intercalated with a non-magnetic tunnel barrier. For Fe/MgO tunnelling junctions, Parkin *et al.* [196] and Yuasa *et al.* [197] have shown that GMR ratios can reach in excess of 300 %. Furthermore, theoretical calculations have shown that the conductance is highly sensitive to the position on the transverse Brillouin zone [145]. In particular, minority spins present high conductance in small regions away from the Γ point and low conductance everywhere else in the BZ.

The same argument used for molecules in the introduction can be applied here. That is, at such a small scale the BZ collapses into a single point. Hence, by appropriately tailoring the MPC, we can probe different points in the BZ and considerably increase the GMR (possibly reaching HGMR values).

Hence we must answer the question of whether the 1D NiO wire is still insulating. If that is the case, then we also need to address the possibility of finding HGMR for this system.

We can start our analysis by using simple LSDA. As it was done with the impurity-free Ni MPC, we also need to find the most energetically favourable arrangement for the device. Using the same method already discussed, *ab initio* atomic relaxations are performed on the system presented in figure (3.9). Whilst the ba-

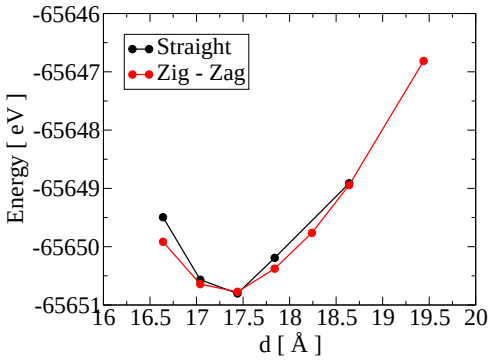

Figure 3.10: Total energy curves using LSDA for different tip separations of a nickel point contact with one oxygen atom between the tips. We started from two different configurations, a straight configuration (black curve) in which the oxygen atom lies along the axis of the two pyramids and a zig-zag configuration (red curve) where the oxygen is initially displaced from the axis. Note that there is a single energy minimum independent of the starting configuration.

sis set for Ni is the same as the previous calculation we use a double-ζ basis with polarisation for oxygen s and p orbitals.

We performed our calculations with two different initial arrangements of the oxygen atom. In the first case we placed the oxygen atom along the axis of the two pyramids while in the second it was displaced perpendicular to the axis. In both configurations the oxygen atom as well as some of the Ni atoms were allowed to relax to their preferred arrangement. The total energy curve as a function of the elongation (distance d between the bases of the two pyramids) is shown in figure (3.10). Despite initially different, at the energy minimum (d = 17.04 Å), both arrangements have an energy minimum for a straight configuration. In contrast, at smaller separations (compressive strain), in order to obtain better bond distances, the oxygen atom prefers a zig-zag arrangement.

By using the atomic positions at the energy minimum we proceed to calculate the zero-bias conductance which are shown in figure (3.11). The transmission coefficients for the PA configuration show a high conductance for the minority and low conductance for the majority spins (approximately 0.5 G_0 and 2.5 G_0 respectively). This is clearly an indication that we have suppressed part of the contribution to the conductance close to E_F which come from the s states.

In the AA the majority and minority spins are identical given the mirror-symmetric nature of the system (see figure (3.11b)). The conductance in this case is equal to $G^{\uparrow} = G^{\downarrow} = 1.75\ G_0$. The overall conductance is larger in the antiparallel case which in turn yields a negative magnetoresistance ratio of approximately -6.3 % .

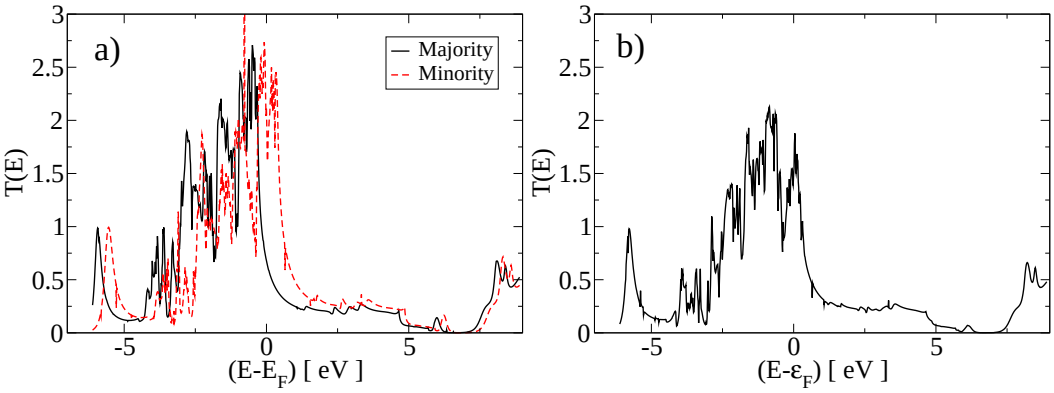

Figure 3.11: Zero bias transmission coefficients of Ni point contacts with oxygen in the LDA approximation for a) parallel and b) anti-parallel cases. The solid (dashed) lines represent the majority (minority spins). In the anti-parallel case, due to the mirror symmetry of the MPC, the transmission coefficients for majority and minority spins are identical.

Although we have shown that the s orbitals seem to be partially removed from the region around E_F, the desired insulating behaviour, specially for the AA case, seems to be still missing. At first, it might seem that the prospect of MPC-based tunnelling devices is dreary. However one must remember that LDA fails in describing bulk NiO correctly and one needs a different exchange and correlation functional.

3.2.4 Effects of different exchange-correlation potentials (V_{XC}) for oxygen-rich Ni point contacts

We have shown earlier (see section (2.2.1)) that the LDA+U is a much more appropriate exchange and correlation functional to treat bulk NiO. It is only natural to use the same method with a one-dimensional NiO chain. In this case correlation effects are very likely enhanced by low-coordination (2-fold instead of the 6-fold in bulk NiO).

We have also shown, in section (2.5.2), that the band structure of an infinite chain can give some insight into the character of the transport properties in quantum point contacts (albeit the final transmission coefficients are given by a combination of factors including the alignment of the Fermi energy and the coupling to the electrodes). Therefore, we can start exploring the Ni-O-Ni tip shown in figure (3.9) by looking at a one-dimensional infinite NiO chain.

We performed calculations using both LDA and LDA+U for an infinite NiO chain with a fixed Ni-O distance of 1.8 Å. Let us first focus on the LDA. Our results for the band structure and PDOS for these two alignments are shown in figure (3.12). The

total energy difference between these two configurations is small, *i. e.*, the chain is not magnetic. Furthermore, in both cases we see a metallic behaviour corroborating the results obtained for the transmission coefficients of the MCP (Fig. (3.11)).

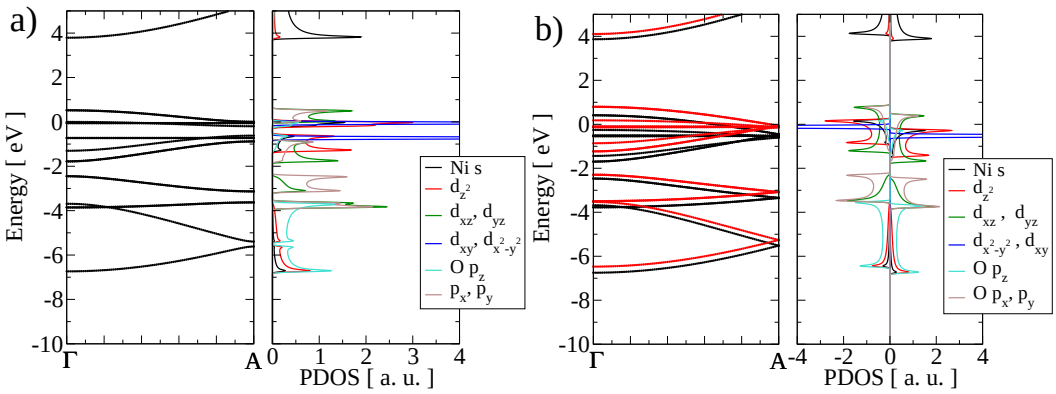

Figure 3.12: Band structures (left panels) and projected density of states (right panels) for an infinite one-dimensional NiO wire using LDA in the (a) antiferromagnetic and (b) ferromagnetic alignments. Black (red) lines indicate majority (minority) spin bands. In the AA case majority and minority spin bands and the projected density of states are identical.

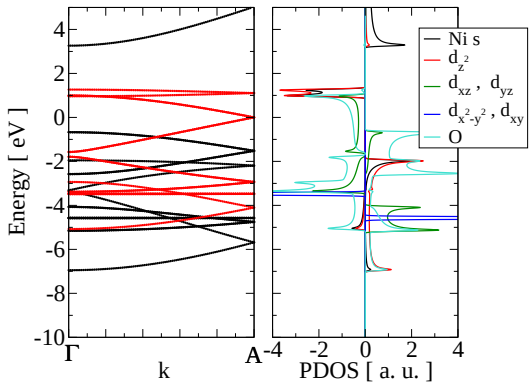

Figure 3.13: Band structures (left hand-side panel) and projected density of states (right hand-side panel) for an infinite one-dimensional NiO wire using LDA+U in the ferromagnetic alignment. The values of U and J are set to 6 eV and 1 eV respectively.

The electronic structure of the nanowire changes significantly with LDA+U. For the ferromagnetic alignment the band structure shown in figure (3.13) is that of a half-metal, *i.e.*, the majority spin states are completely filled and do not present DOS at $E - F$. Therefore the band-structure is that of an insulator. In contrast the minority spin bands lie close to the Fermi level and are partially filled. Differently

from the pure nickel chain there is no signature of the s band around E_F. The Fermi surface is mostly due to oxygen p and Ni d_{xz} and d_{yz}.

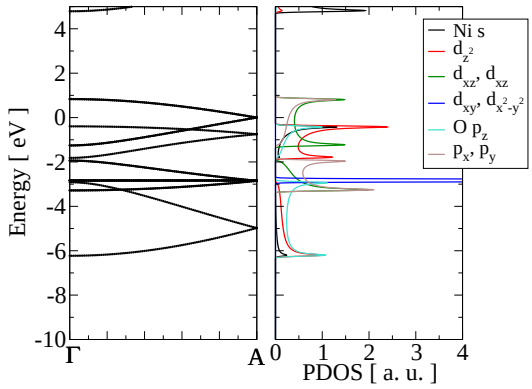

Figure 3.14: Band structures (left hand-side panel) and projected density of states (right hand-side panel) for an non-magnetic infinite one-dimensional NiO wire using LDA+U. The values of U and J are set to 6 eV and 1 eV respectively. Majority and minority spin bands are identical.

However, the lowest energy configuration (in LDA+U) for an infinite NiO chain is non-magnetic.[5] This means that the occupation in each Ni atom for up and down spins is identical. The band structure and PDOS for this solution are shown in figure (3.14) and it is clearly metallic.

Finally, if starting from the anti-ferromagnetic alignment, we will observe that the results are very sensitive to the initial choice of orbital occupation. The results which are shown in figure (3.15) range from an insulator to a conductor.[6] The band structure for the insulating AF nickel oxide wires is similar to those obtained using all-electron density functional theory with the B3LYP exchange-correlation potential.[7] It was not possible to converge the conducting system with this latter functional.

When we attach the pyramids to the chain to form the MPC we are unable to converge the non-magnetic solution. The much larger pyramids which resemble bulk Ni, and therefore magnetic, strongly influence the two Ni atoms forming the chain. Hence, the final configuration can only be either the PA or AA the configuration.

[5]The non-magnetic solution is the most favourable one for a range of values of U ranging from 2 eV to 8 eV (J was kept constant at 1 eV).

[6]For an 1D system one would expect that a Peierls [198] distortion gives rise to a gap at the Fermi level and consequently prevents a conducting state to appear. Here we are only considering a hypothetical scenario in order to compare with the real transport calculations where the electrodes break translational symmetry and a conducting state becomes possible.

[7]The calculations were performed using CRYSTAL 2003 [199] and the all-electron basis sets provided in [200, 201].

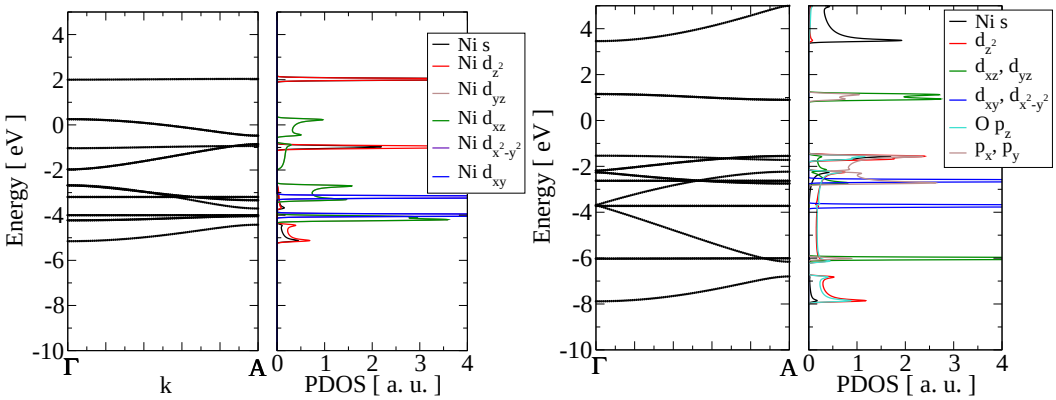

Figure 3.15: Band structures (left hand-side panel) and projected density of states (right hand-side panel) for an infinite one-dimensional NiO wire using LDA+U with anti-ferromagnetic alignment. a) Metallic and b) insulating solutions. The values of U and J are set to 6 eV and 1 eV respectively. We have used different starting orbital occupations for these antiferromagnetic calculations.

The transmission coefficients calculated using LDA+U are shown in figure (3.16). For the PA configuration we can see a qualitative agreement with the LDA case (figure (3.11a)). The transmission for minority spins is slightly higher and that for majority spins is lower ($\sim$ 0.2 G_0). The majority d states are shifted downwards compared to the LDA case and although the transmission coefficients at E_F are non-zero, it does resemble the half-metal behaviour observed for the infinite chain. For the AA we have chosen to work with the insulating state. In that case a completely different picture arises: the conductance for both parallel and antiparallel is approximately 0.2 G_0 because the s states are driven away from the Fermi energy. The resulting magnetoresistance reaches the much higher value of 450 %.

Recently calculations using B3LYP [202] in oxygen-rich MPC's have shown GMR ratios of approximately 600 % . The discrepancy in the results are probably due to differences in the anti-parallel configuration. The authors of the aforementioned work use the B3LYP functional on all the atoms of the point contact although it has been shown to over-correct the properties of bulk Ni resulting in a considerably larger magnetic moment when compared to the experimental value. Furthermore, they also describe the electrodes using a model Hamiltonian which can lead to extra scattering processes when one tries to match the leads' self-energies to the pyramids [82]. In metallic systems that is not so important, but in the tunnelling regime small differences in the electronic structure might lead to large changes in the conductance. Nevertheless, these results are within the same range as those from our calculations.

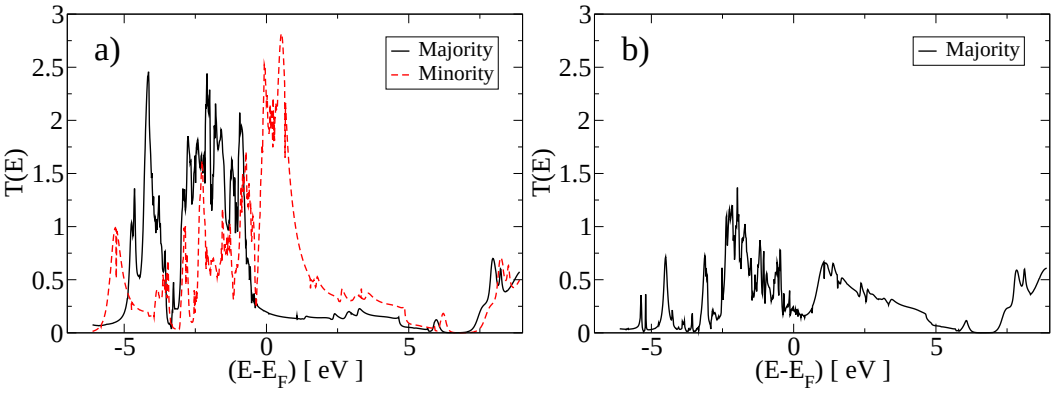

Figure 3.16: Zero bias transmission coefficients of Ni point contacts with oxygen in the LDA+U approximation for a) parallel and b) anti-parallel cases. The solid (dashed) lines represent the majority (minority spins)

3.3 Conclusion

In summary, in this chapter we have studied different aspects of magnetic point contacts and their applications as possible electronic devices. We have investigated, using NEGF's within a tight-binding approach, rôle of the position of the DW inside the junction and its effect on the I-V curves. Our main result is that largely asymmetric I-V curves can be found when the DW is asymmetrically placed inside the point contact, although the whole structure does not present any structural asymmetry. We have interpreted this result in terms of the charging properties of the junction and of spin-dependent HOMO/LUMO alignment. This asymmetric behaviour can only be obtained using a non-equilibrium approach to transport.

We have also studied MPCs using a more accurate DFT approach. Using *Smeagol* we addressed the issue of LGMR and HGMR in atomically sharp MPCs. In the case of impurity-free Ni MPCs we observe higher MR ratios when we use the LDA+U exchange and correlation functional. These results are comparable to calculations performed on similar systems [194, 195]. However, the observed increase is not able to account for HGMR (MR in excess of 10,000 %). We have speculated about the presence of oxygen impurities in the constriction forming an atomic size NiO tunnel barrier. In this case the use of LDA+U considerably changes the picture. For the benchmark structure formed by a NiO infinite chain LDA gives a metallic state for both PA and AA, whereas this may become insulating with the inclusion of corrections to the exchange and correlation functional. The magnetoresistance increases considerably to values close to 500 %.

This result is still at least one order of magnitude smaller than experimentally

observed values [194, 195]. From our calculations we must conclude, at least for the configurations that were studied here, that HGMR can not possibly originate solely from electronic means in contrast to what has been previously suggested [163].